

First-results from the Perseverance SHERLOC investigation: Aqueous alteration processes and implications for organic geochemistry in Jezero crater, Mars E. L. Scheller¹, J. Razzell Hollis², E. L. Cardarelli², A. Steele³, L. W. Beegle², R. Bhartia⁴, P. Conrad³, K. Uckert², S. Sharma², B. L. Ehlmann¹, S. Asher⁵, E. L. Berger⁶, A. S. Burton⁷, S. Bykov⁵, T. Fornaro⁸, A. C. Fox⁹, M. Fries⁷, L. C. Kah¹⁰, T. Kizovski², F. M. McCubbin⁷, K. Moore², R. Roppel⁵, S. O. Shkolyar¹¹, S. Siljeström¹², A. J. Williams¹³, B. Wogsland¹⁰, R. C. Wiens¹⁴, and the SHERLOC team. ¹Division of Geological and Planetary Sciences, California Institute of Technology, CA (eschelle@caltech.edu). ²Jet Propulsion Laboratory, California Institute of Technology, CA. ³Earth and Planets Laboratory, Carnegie Institution for Science, DC. ⁴Photon Systems Incorporated, CA ⁵Department of Chemistry, University of Pittsburgh, PA. ⁶Texas State University - Jacobs JETS - NASA Johnson Space Center, TX. ⁷NASA Johnson Space Center, TX. ⁸INAF-Astrophysical Observatory of Arcetri, Italy. ⁹NASA Postdoctoral Program - NASA Johnson Space Center, Houston, TX. ¹⁰Department of Earth and Planetary Sciences, University of Tennessee, TN. ¹¹NASA Goddard Space Flight Center, MD, ¹²RISE Research Institutes of Sweden, Sweden, ¹³Department of Geological Sciences, University of Florida, FL. ¹⁴Los Alamos National Laboratory, NM.

Introduction: The Perseverance rover landed in Jezero crater, a site selected to fulfill the Mars-2020 mission goals of characterizing the geology of habitable environments and searching for signs of life while collecting samples for return to Earth [1]. Jezero hosted an open-basin lake during the late Noachian/early Hesperian (~3.7 Ga) [1-2], has units associated with the largest carbonate deposit identified on Mars [3-4], and has a well-preserved delta with clay and carbonate-bearing sediments, well-suited to preservation of organics [1,3-4]. Investigating the nature of organics and aqueous environments within their geologic context allows us to understand important aqueous processes and determine habitability within Jezero crater. Previous *in situ* landed measurements of organics could not resolve their spatial and mineralogical context [5-6]. Although Martian meteorites lack geological context, the spatial distribution of organic compounds in Martian meteorites have allowed recognition of an association between aqueous processes and organics [7-8]. Here, we show for the first time in-situ associations between carbonate-forming ultramafic alteration process, later stage aqueous sulfate and perchlorate formation, and organics on the Martian surface.

Methodology and geological context: We use the Perseverance rover's SHERLOC instrument (Scanning Habitable Environments with Raman and Luminescence of Organics and Chemicals), a deep-ultraviolet fluorescence and Raman scattering spectrometer capable of mapping the organic and mineral composition with a spatial resolution of 100 μm resolution to report the presence of organics and aqueously formed minerals at Jezero crater [9]. These spectral detections were compared with co-located images obtained with the autofocus context imager (ACI) and the WATSON camera for textural analysis [9]. As of writing, the Perseverance rover has abraded five targets that were measured with the SHERLOC instrument. The five targets are located in two different orbitally-identified geological units within the floor of Jezero crater; the

Crater Floor Fractured Rough unit (CF-Fr) and the Séítah region within the Crater Floor Fractured 1 unit (CF-F1) [10]. In orbital infrared spectroscopic data, the CF-Fr unit is associated with pyroxene spectral signatures and minor alteration, while the Séítah region is associated with olivine and minor Mg-rich carbonates and clays [3-4,10].

Carbonation of ultramafic protolith recorded within Jezero crater: All scans of abraded targets within the Séítah region reveal strong peaks at 1080–1090 cm^{-1} consistent with carbonate and peak singlets or doublets at 820–840 cm^{-1} attributed to olivine (Fig. 1), consistent with orbital infrared observations. Our detailed micron-scale petrographic and spectroscopic evidence shows that these carbonates formed through carbonation of an ultramafic protolith. The supporting observations include: (1) Carbonate cation compositions match those of olivine, suggesting mixed Fe- and Mg-olivine gave rise to mixed Fe- and Mg-carbonates, similar to observations of ultramafic systems on Earth and within Martian meteorites [3-4,7-8]. (2) The observed carbonates co-occur with hydrated materials, gypsum, and potentially aqueously-formed phases, amorphous silicates and phosphate. (3) The spectral and textural variation of olivine and carbonate dominated zones and olivine-carbonate mixtures within both primary grains and interstitial zones are expected for carbonated ultramafic protoliths. (4) These mineral associations and textures closely resemble those observed within the ALH84001 and Nakhilite meteorites attributed to olivine carbonation on Mars [6-7]. Taken together, micron-scale SHERLOC documentation of these phenomena bridge previous orbital and meteorite observations and demonstrate in-situ regionally extensive (~10⁶ km²) ultramafic alteration resulting in geological deposition of carbonates. Furthermore, we observe that olivine carbonation was involved in preserving and possibly synthesizing organics, which makes this environment potentially habitable, as previously suggested in [1,3-4] (Fig. 1).

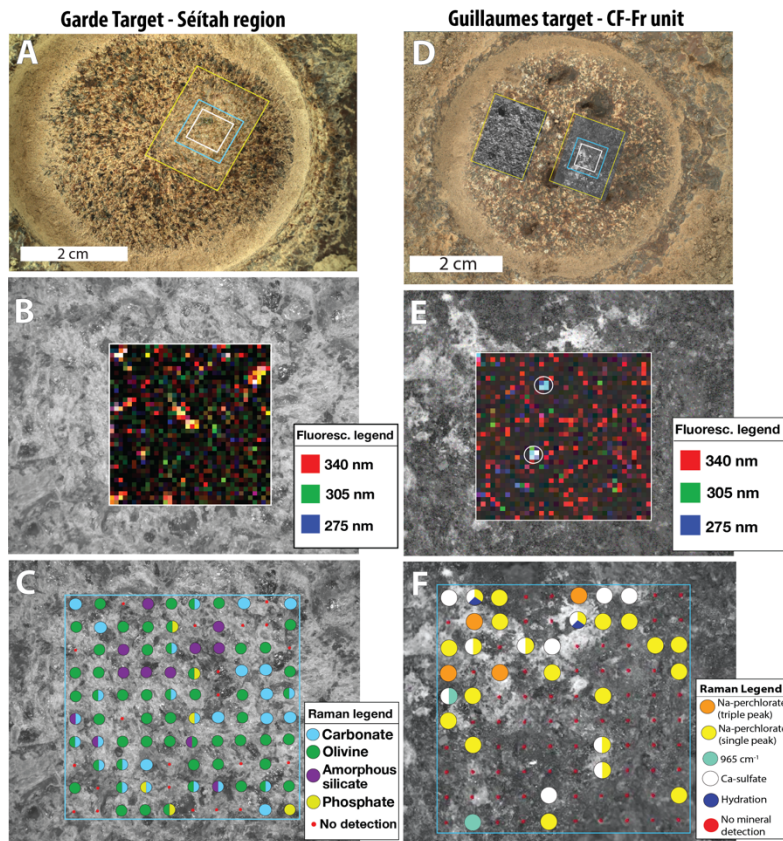


Figure 1: (A-C) Figures of Garde target from the Séítah region. (A) WATSON image of Garde abrasion target. Yellow rectangle shows position of grey-scale context image in panel B-C. Blue and white rectangle shows fluorescence and Raman scans. (B) Fluorescence intensity map showing features related to organics. (C) Map of mineral detections interpreted from Raman spectra. (D-F) Figures of the Guillaumes target from the CF-Fr unit. (D) WATSON image of Guillaumes abrasion target. Yellow rectangle shows position of grey-scale context image in panel B-C. Blue and white rectangle shows fluorescence and Raman scans. (E) Fluorescence intensity map showing features related to organics. White circles show organics related to Supercam laser shots, while the rest are inherent to the rock. (F) Map of mineral detections interpreted from Raman spectra.

Late-stage aqueous perchlorate and sulfate in Jezero crater: An abrasion target within the CF-Fr unit contains combinations of high intensity $950\text{--}955\text{ cm}^{-1}$ peaks and minor $1090\text{--}1095\text{ cm}^{-1}$ and $1150\text{--}1155\text{ cm}^{-1}$ peaks that are spectral fits to anhydrous perchlorate (Fig. 1). Some spectra show a combination of $950\text{--}955\text{ cm}^{-1}$ peaks with equally strong $1010\text{--}1020\text{ cm}^{-1}$ peaks, low intensity broad features at 1120 cm^{-1} , and occasional broad 3450 cm^{-1} hydration (-OH) features, indicating a mixture of Ca-sulfate and perchlorate that is minimally hydrated (Fig. 1). The detections of perchlorates within Jezero crater differ from previous measurements (e.g. Phoenix lander, Curiosity rover, Tissint meteorite [7,11]) because they are observed to be intimately related to aqueous processes including sulfate formation, they present as a secondary white void-fill occurring within the interior of the rock, and they are found to likely be Na-perchlorate.

Organics in Jezero Crater and implications for their formation:

Three different types of organics embedded within three different lithologies were observed within the abraded targets. Organics associated with low intensity $\sim 340\text{ nm}$ fluorescence were widespread within targets with no apparent association to particular minerals (Fig. 1). Organics associated with $\sim 305\text{ nm}$ and $\sim 275\text{ nm}$ fluorescence correlated with sulfates within the Bellegarde target in the CF-Fr unit, while organics associated with high intensity $\sim 340\text{ nm}$ fluorescence correlated with carbonate, phosphate, and amorphous silicate mixtures within the Garde target in the Séítah region (Fig. 1). Although assignment of fluorescence signatures to specific organic compounds is not conclusive, $\sim 340\text{ nm}$ fluorescence is generally more consistent with 2-ring aromatic organics, $\sim 275\text{ nm}$ fluorescence is more consistent with 1-ring aromatic organics, and $\sim 305\text{ nm}$ fluorescence can be created by either 2- or 1-ring aromatics [12]. These observations indicate that the strongest fluorescence signatures interpreted as organics were found in materials associated with aqueous processes, i.e. sulfate- and carbonate-bearing materials, suggesting both brines and ultramafic carbonation aqueous environments were capable of preserving organics on ancient Mars. In

Martian meteorites, simple aromatic organics proposed to have been synthesized through aqueous processes can be found within minerals associated with olivine carbonation and in spatial association with perchlorate and sulfate materials [7-8], similar to SHERLOC observations. Hence, we advance an abiotic aqueous synthesis origin for the organics although we cannot rule out the presence of organics from meteoritic in-fall or putative organic biosignatures. Detailed analyses will be required upon return of these materials to Earth.

Acknowledgments: Thanks to the Mars-2020 team for efforts to collect the data. E.L.S. was supported by NESSF #80NSSC18K1255 to B.L.E. **References:** [1] Farley, K. A. et al. (2020) *Space Sci. Rev.* 216, 1-41. [2] Fassett C. I. & Head J. W. (2008) *Icarus* 198, 37-56. [3] Goudge T. A. et al. (2015) *JGR: Planets*, 120, 775-808. [4] Ehlmann, B. L. et al. (2008) *Science* 322, 1828-1832. [5] Navarro-González R. et al. (2010) *JGR: Planets*, 115, E12. [6] Eigenbrode J. L. et al. (2018) *Science*, 360, 1096-1101. [7] Steele A. et al. (2018) *Sci. Adv.*, 4, eaat5118. [8] Steele A. et al. (accepted) *Science*. [9] Bhartia R. et al. (2021) *Space Sci. Rev.*, 217, 58. [10] Stack, K. M. et al. (2020) *Space Sci. Rev.*, 216, 1-47. [11] Martin, P. E. et al. (2020) *JGR: Planets*, 125. [12] Bhartia R. et al. (2008) *Appl. Spectrosc.*, 62, 1070-1077.